Multi-scale, Mechano-biological Model of Nanoparticle Toxicity

Jerry Jenkins, Kapil Pant, Jonathon Hood, and Shivshankar Sundaram
CFD Research Corporation
215 Wynn Drive, Huntsville, AL 35805
Email: sxs@cfdrc.com

ABSTRACT

Comprehensive assessment of the toxic physiological effects of short and long term exposure to nanoparticles requires a detailed understanding of particle deposition and partitioning within the body (the "dose"), and the inflammatory cellular "response" to the dose. In this paper, we report on the progress towards the development of an integrated computational architecture for the assessment of nanoparticle toxicity. The simulational methodology uniquely couples mixed-dimensional spatio-temporal models of nanoparticle dispersion with quantitative, dynamic models of cellular response. Critical elements of the modeling framework are demonstrated for nanoparticle inhalation via the pulmonary route. Results for aerosol deposition and dispersion in fully 3D models derived from medical imaging data as well as 1D model of stochastically generated tracheobronchial tree are presented. At the cellular level, particle chemical properties are used to yield predictions of the dynamic cellular – oxidative, inflammatory and apoptotic – response to the received dose.

Keywords: nanoparticle, toxicity, assessment, cellular response, deposition, modeling, simulation

1 INTRODUCTION

The development of effective countermeasures to combat toxic physiological response to nanoparticle exposure is vital for civilian (environmental pollutants), military (diesel exhaust particles, and other battlefield contaminants) as well as space applications (lunar and martian dust). The adverse effects of nanoparticle exposure can range from mild illness to mortality. Even at low, non-toxic levels, untreated exposure may lead to pathological complications in the long-term. The primary mode of systemic delivery of nanoparticles is via the respiratory route, although ingestion can occur upon contamination of food/water resources. As a result of inhalation following exposure, both short-term (pulmonary structure and function) and long-term (silicosis like) effects are likely. Exposure risk depends on a multitude on confounding factors such as, particle physical (respirability) and chemical (toxicity) properties, particle concentration, exposure time, individual's respiratory health and genetic make-up, etc. Therefore, accurate assessment of nanoparticle toxicity calls for sound knowledge of particle deposition in various regions of the body (the "dose") as well as detailed understanding of the cellular "response" to this deposited dose.

Accurate quantitative prediction of the amount of internal and external deposition on the body (lung, skin, sinuses, eyes, etc.) is critical to setting the nanoparticle dose. For example, nanoparticle deposition in the lung is site-specific and depends, among other factors, upon the aerodynamic size, electrostatic charge distributions and gravitational forces [1]. Once inhaled, nanoparticles can be expunged via mucociliary clearance over a relatively short period or reach the sensitive alveolar regions and stay for long times [2]. Therefore, it is necessary to describe nanoparticle deposition in the body using spatio-temporal models. Given the deposited dose, models describing cellular response to nanoparticle contact can be used to determine the level of inflammation. Cellular nanoparticle toxicity is primarily due to the generation of Reactive Oxygen Species (ROS) through a series of complex cyclical intracellular chemical reactions that result in the production of the superoxide and hydroxyl ions. Currently, there are no modeling platforms that enable the prediction of the multi-scale physiological toxic response to nanoparticle exposure.

In this paper, we present a simulation methodology for quantitative prediction of physiological toxic response to nanoparticle exposure. Since the primary mode of nanoparticle exposure is via the respiratory system, we focus on *pulmonary* toxicity assessment. At the organ level, spatio-temporal models are utilized to take into account nanoparticle properties and physiological parameters to predict regional deposition. At the cellular level, particle chemical properties are used to yield predictions of the dynamic cellular response to the received dose.

2 METHODS

2.1 Lung Morphology

Recent advances in medical imaging modalities such as Computed Tomography (CT), specifically High-Resolution CT (HRCT), have made it possible to capture upper airway geometries with adequate physiological fidelity. The lower airways, on the other hand, are unresolved even by the most sophisticated imaging techniques available. However, the isotropy of lung morphology at the lower airway levels may be used to generate a stochastic, fractal structure. We exploited this fact to develop a simulation environment for integrative computational modeling of the airways. The computational domain for the calculations presented in this paper was generated using (1) a 64-slice CT scan data

(anonymized) to obtain upper airway geometry, and (2) a stochastic algorithm was developed to "complete" the lung structure down to the desired generation number.

2.2 Deposition Modeling

Physics-based numerical simulations have been successfully employed by several researchers to analyze flow and particulate dispersion in physiologically derived pulmonary pathways. However, most of the studies to date have focused on microparticle deposition in the oropharyngeal region or on the early bronchial branching (4-6 generations, [3, 4]). Transport and deposition in the deep lung region has heretofore been attempted only in the context of simplified network models with large empirical content [5]. In contrast, the present computational models focus on a mixed-dimensional methodology with advanced physical and numerical models for prediction of lung deposition. Traditionally studied microparticles, compared with nanoparticles, behave in a significantly different manner in their dispersive and depositional behavior [6] and this is an added emphasis in this study. The conservation equations are solved using appropriate descriptions, viz. fully 3D for upper airways and 1D for lower airways, to compute airflow and particle dispersion.

In the upper airways (3D), turbulent airflow is solved using traditional Reynolds Averaged Naviér-Stokes (RANS) methods. Particle dispersion and deposition is modeled using traditional Lagrangian (trajectory) methods [7]. Airflow in the lower airways was solved using CFDRC-developed 1D methodology [8]. In this approach, airways are represented by a tubular structure (called "Filament"). A finite-difference formulation is employed to solve for fluid flow. In 1D, steady state the conservation of mass and momentum reduce to:

$$\Delta(\rho A v)=0 \quad \Delta(\dot{M} v)=\bar{A}\Delta p-\tau_W P\Delta x+\rho g\Delta x \qquad (1)$$

where ρ is the fluid density, A is the Filament cross-sectional area (bar denotes averaging over the length Δx), P is the perimeter, $\dot{M}$ is the mass flux, p is the pressure, τ_w is the wall shear stress and g is the acceleration due to gravity.

Particle transport in lower airways was simulated in an Eulerian framework. Scalar transport in the 1D framework is solved using a convective-diffusive formulation:

$$\Delta(\dot{M}\phi)=\Delta(D\Delta\phi)+S_\phi \qquad (2)$$

where D is the mass diffusion coefficient of the scalar variable and S_ϕ is the sink term. The mass diffusivity of the particles was computed using the Stokes-Einstein relation. The sink term for aerosol transport in Filament formulation was supplied using stochastic particle deposition models. The overall particle deposition probability in the tubular region is governed by the deposition probabilities due to impaction, sedimentation and, particularly relevant for nanoparticles, Brownian diffusion [9]:

$$P_{D,\text{Impaction}} = 1-\frac{2}{\pi}\cos^{-1}(y)+\frac{1}{\pi}\sin[2\cos^{-1}(y)]$$

$$P_{D,\text{Sedimentation}} = 1-\exp(-\frac{4gC_C\rho_p r_p{}^2 L\cos\phi}{9\pi\mu R v}) \qquad (3)$$

$$P_{D,\text{Brownian}} = 1-\sum_{i=1}^{3} a_i \exp(-b_i x)-a_4\exp(-b_4 x^{2/3})$$

Here $x = LD/2R^2v$ and $y=\theta*\text{St}$, where D is diffusion coefficient, R is tube radius, L is tube length, v is mean flow velocity, ϕ is angle relative to gravity, θ is branching angle, μ is fluid viscosity, St is Stokes number, ρ_p is particle density, r_p is particle radius and C_C is Cunningham correction factor. The coefficients in Equation (3) are a_1=0.819, a_2=0.0976, a_3=0.0325, a_4=0.0509, b_1=7.315, b_2=44.61, b_3=114 and b_4=79.31.

2.3 Toxicity Modeling

Airway toxicity of airborne contaminants has long been investigated in the environmental pollution community. A well-studied contaminant is Diesel Exhaust Particulates (DEP). Adsorption of DEP onto the surface of an alveolar macrophage (AM) causes the AM to phagocytose the DEP. Once inside the AM, the chemicals (polycyclic aromatic hydrocarbons (PAHs), halogenated aromatic hydrocarbons (HAHs) and quinones [10]) on DEP surface desorb and undergo xenobiotic metabolism in a two-step process: (1) oxidation, reduction or hydrolysis by enzymes to render the xenobiotic non-toxic, and (2) catabolism or secretion of the non-toxic compound. Xenobiotic metabolism can produce a significant amount of Reactive Oxygen Species (ROS) such as, hydrogen peroxide, which mediate cellular toxicity.

Excess ROS can also activate AM, which can induce acute physiological effects. Cytokines release from alveolar macrophages under heavy oxidative load causes a variety of local pulmonary responses (Figure 1). Studies have shown that increased ROS load increases macrophage production of interleukins and TNF-α necessary for the recruitment and activation of B cells, mast cells and eosinophils High levels of oxidative stress on AMs can release reactive oxygen intermediates such as, nitric oxide, leukotrienes, and platelet activation leading to cytotoxicity and smooth muscle contraction. B cell activation of mast cells induces the release of histamines, leukotrienes and prostaglandin D2, which can lead to increased mucous secretion, nerve irritation, cough, bronchial hyperresponsiveness and serum leakage. Chronic exposure to agents which induce high levels of oxidative stress, can ultimately lead to bronchial and epithelial damage and bronchial hypersensitivity. In the absence of detailed biological studies on the cellular mechanisms of nanoparticle toxicity, it can be reasonably expected that many of the phenomena described above will be implicated strongly in the biological effects of nanoparticle exposure. Thus it can be inferred that cellular response to nanoparticle exposure is determined by a complex network of intracellular reaction pathways stimulated by oxidative and inflammatory stresses with the

outcome (reduced function, apoptosis) determined by the strength of anti-oxidant and anti-inflammatory responses.

In past research, we have developed/adapted algorithms specifically designed to address the problems of dynamic pathway simulation, pathway identifiability/verifiability, and kinetic coefficient estimation for large-scale signaling networks. Dynamic simulations of intracellular reaction pathways are performed using deterministic or stochastic (modified Gillespie) algorithms. Parameter extraction and validation of pathway models are performed using a finite time horizon State Regulator Method (SRM) [12].

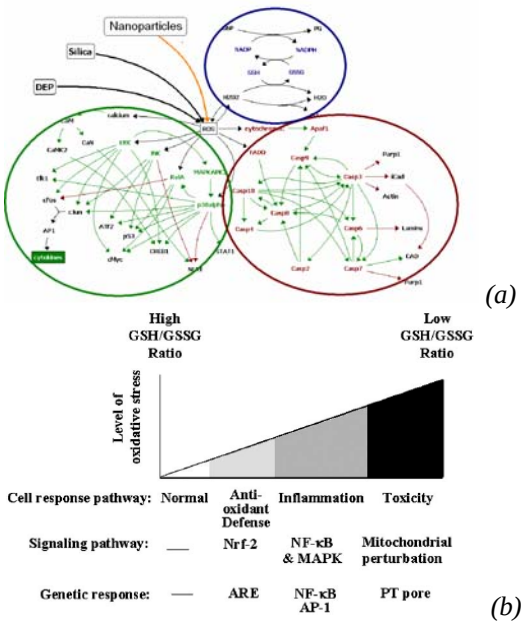

Figure 1. (a) Intracellular reaction pathways illustrating the effects of reactive oxygen species on the alveolar macrophage; blue-antioxidant, green-inflammatory, red-apoptotic (b) Differential response of alveolar macrophages to increased oxidative stress [11]

3 RESULTS & DISCUSSION

The Upper Respiratory Tract (URT) and the upper airways (Generation 2-6) were generated by processing anonymized medical imaging data. A 64-slice CT scan data was segmented using a thresholding algorithm to generate a 512×512×741, 8-bit data set (Figure 2a). The data was then analyzed and processed using customized macros/widgets to generate a surface rendering of the airway structure. The surface was triangulated and exported in stereolithographic format to allow computational mesh generation (Figure 2b).

The lower airway computational domain (shown in Figure 3) was created by (a) importing a root tree configuration in the lobar regions, and (b) space-filling the lobar volume using a stochastic branching algorithm. The branching algorithm used in the present study was based on stochastic sampling of Probability Distribution Functions (PDFs) of the following physiological parameters: (a) length-to-diameter ratio, (b) daughter-to-parent-diameter ratio, (c) branching angle, and (d) rotation angle.

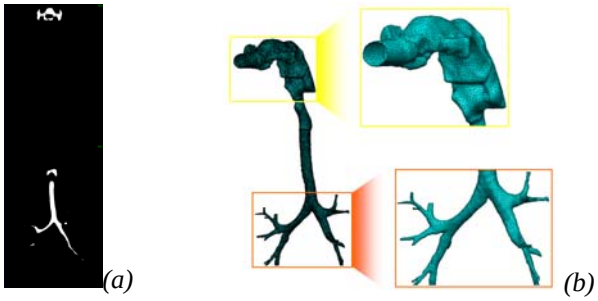

Figure 2. Image processing for upper airway computational domain creation (a) Coronal slices of medical imaging data set (b) Computational mesh (~656,000 tetrahedral cells)

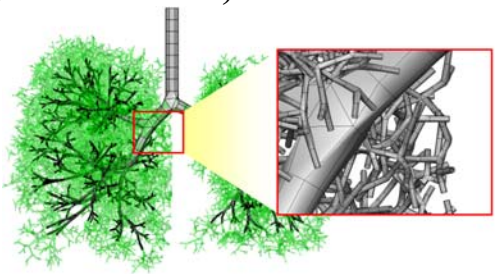

Figure 2. Lower airways computational domain creation. Daughter airways (green), ending in terminal bronchioles, were spawned from a "root" tree (black).

Airflow and aerosol dispersion simulations were performed in the imaging based integrated URT and upper airway geometry. Calculations were also carried out in idealized (Weibel) geometries for comparison. Simulations were carried out at inhalational flow rates of 12.5 and 28.3 L/min (sedentary and light activity). An aerosol bolus containing particles in the size range of 500 nm to 25 μm was released at the mouth. The deposition efficiency of the aerosol particles is shown in Figure 3a. The particles are grouped into nanoparticles and microparticles, based on size. Note that a significant amount of nanoparticles pass through the upper, conducting airways and are eventually deposited in the deep lung. The overall deposition efficiency in the oropharynx, the tracheobronchial region and Generation 1-4 is plotted in Figure 3b. In general, the deposition in the idealized geometry is under-predicted, prominently so in the oropharyngeal region. These calculations clearly underscore the need for the use of physiologically realistic geometries for prediction of particle deposition in the respiratory system.

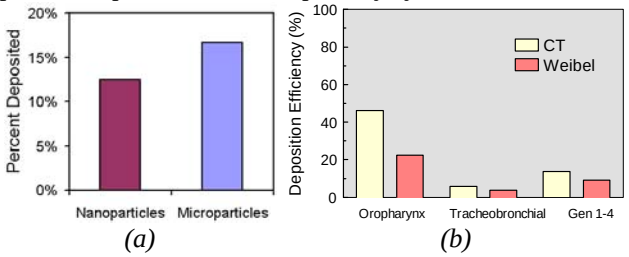

Figure 3. (a) Deposition efficiency of nano- and micro-particles in upper airways (b) Particle deposition in image-based and idealized airway geometry.

Since the upper airway simulations clearly demonstrate that nanoparticles need to be tracked in the lower airways to predict the deposited dose accurately, a 10 generation tracheobronchial tree was constructed. Particles exiting the upper airways were "patched on" to this tree and aerosol fate in the deep lung was tracked using the methodology described in §2. As in the upper airway simulations, aerosol representative of nano (500nm) and micro (10μm) particles was released at the trachea and lung ventilation maps were generated. Aerosol concentration contours (which can be correlated to the deposition fraction) in the tracheobronchial tree for different particle sizes is presented in Figure 4. Low concentration is shown in blue and high concentration is depicted by magenta. Note that the 10μm particles, which are larger than respirable micro-particles, fail to traverse to the deep lung due to impaction and deposition is localized to the upper airways. Nanoparticles on the other had are able to penetrate deep into the lung, with only small depositional losses in upper airways.

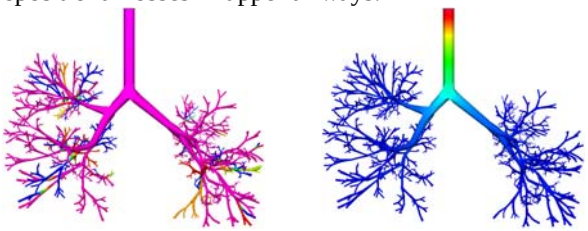

(a) *(b)*

Figure 4. Aerosol concentration contours in 10-generation tracheobronchial tree (a) Nanoparticles (b) Microparticles.

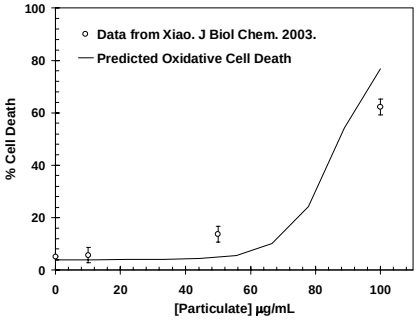

Figure 5. Dose response curve for ROS induced cell death as a function of diesel exhaust particle loading concentration. Model predictions are compared with experimental data reported by [11].

Local (generation specific) deposition of nanoparticles, estimated using the above simulations, is used as input to simulate cellular response. Quantitative, dynamic simulations based on a subset of the cellular mechanisms discussed earlier were performed. The objective was to study, over the range of nanoparticle deposition, temporal cellular response focusing on the oxidative, inflammatory and apoptotic processes. As seen in Figure 5, our model predicts an increase in oxidative stress with increasing particle loading, indicated by the decrease in the glutathione (GSH/GSSG) ratio. Reduced glutathione (GSH) is a major antioxidant in human tissues that reduces hydrogen peroxide to water catalyzed by glutathione peroxidase. During this process, GSH is oxidized to form GSSG, which is then recycled by glutathione reductase back to GSH. Increasing the oxidative stress on a cell causes the glutathione ratio to decrease as seen in Figure 5. Our models successfully reproduced the experimentally observed dose-dependent increase in cell death as a function of particle loading. These cell death/damage probabilities can be directly correlated, and coupled to the mechanical simulations discussed earlier, to manifest local adverse effects.

4 CONCLUSION

We have developed a unified multi-disciplinary (mechano-biological) multi-scale (oropharynx to alveolar response) approach to predict toxic physiological response to nanoparticle exposure. The computational framework includes (a) integrative lung deposition modeling with medical imaging-based, anatomically detailed upper airway models and stochastic lower airway description, and (b) quantitative, dynamic models of nanoparticle induced cellular response. The primary model outcome are (a) locally varying estimates of nanoparticle deposition coupled to (b) dose-dependent cellular response indicative of adverse effects. Preliminary simulations demonstrate the validity and utility of this novel approach. The model framework presented here can be used to: (a) set knowledge-based (rather than *ad hoc* or empirical) requirements for nanoparticle exposure, and (b) develop effective practices and countermeasures to mitigate adverse health effects. Other applications include pharmaceutical drug development and delivery, personalized medicine and biodiagnostics, and homeland defense applications.

ACKNOWLEDGMENT

This work was supported in part by the National Science Foundation (DMI-0420006). The CT scan data was provided by Prof. Eric Hoffman of the University of Iowa and the 3D computational domain was supplied by Prof. Yiannis Ventikos of the University of Oxford.

REFERENCES

1. Donaldson, K., et al. *Part Fibre Toxicol*, 2005, **2**:1.
2. Peters A., et al. *New Engl J Med*, 2004, **351**:1721.
3. Nowak, N., et al. *Ann Biomed Eng*, 2003, **31**:4.
4. Comer, J.K., et al. *J Fluid Mech*, 2001, **435**:25.
5. Anjilvel, S., et al. *Fundam Appl Toxicol*, 1995, **28**:41.
6. Zhang, Z., et al. *J Comput Phys*, 2004, **198**:178.
7. Pant, K., et al. *Proc Respiratory Drug Delivery VIII*, 2002, Tucson, AZ.
8. Pindera, M.Z., et al. *Proc. SPIE 2000*, 2000, **4019**:272.
9. Yeh, H.C., et al. *Bull Math Biol*, 1980, **42**:461.
10. Riedl, M., Diaz-Sanchez, D. J. Allergy Clin Immunol. **115**:221-228 (2005)
11. Xiao, et al. *J Biol Chem*, 2003, **278**:50781.
12. Gadkar, K., et al. *Systems Biology*, 2005, **2**:17.